

## Supplementary Information

# Correlation of nanoscale behavior of forces and macroscale surface wettability

Abhimanyu Rana<sup>a,+#</sup>, Abhijeet Patra<sup>a,b,#</sup>, Meenakshi Annamalai<sup>a,#</sup>, Amar Srivastava<sup>a</sup>, Siddhartha Ghosh<sup>a</sup>, Kelsey Stoerzinger<sup>c</sup>, Yueh-Lin Lee<sup>c</sup>, Saurav Prakash<sup>a,b</sup>, Reuben Yeo Jueyuan<sup>d</sup>, Partho Pattader<sup>d</sup>, Nalam Satyanarayana<sup>d</sup>, Kalon Gopinadhan<sup>a</sup>, Michal M. Dykas<sup>a,b</sup>, Kingshuk Poddar<sup>a,b</sup>, Surajit Saha<sup>a</sup>, Tarapada Sarkar<sup>a</sup>, Brijesh Kumar<sup>a</sup>, Charanjit S. Bhatia<sup>d</sup>, Livia Giordano<sup>c,e</sup>, Yang Shao-Horn<sup>\*c</sup>, T Venkatesan<sup>\*a,b,d,f,g,h</sup>

<sup>a</sup>NUSNNI-NanoCore, National University of Singapore (NUS), Singapore 117411

<sup>b</sup>NUS Graduate School for Integrative Sciences and Engineering (NGS), National University of Singapore (NUS), Singapore 117456

<sup>c</sup>Electrochemical Energy Laboratory, Massachusetts Institute of Technology, 77 Massachusetts Ave, Cambridge, MA 02139, USA

<sup>d</sup>Department of Electrical Engineering, National University of Singapore (NUS), 4 Engineering Drive 3, Singapore 117583

<sup>e</sup>U.S. Department of Energy, National Energy Technology Laboratory, 626 Cochrans Mill Road, P.O. Box 10940, Pittsburgh, PA 15236-0940, USA

<sup>f</sup>Department of Physics, Faculty of Science, National University of Singapore (NUS), Singapore 117551

<sup>g</sup>Department of Materials Science and Engineering, National University of Singapore (NUS), Singapore 117575

<sup>h</sup>Department of Physics, Faculty of Science, National University of Singapore (NUS), Singapore 117551

+Currently at MESA+Institute of Nanotechnology, University of Twente, P.O. Box 217, 7500 AE Enschede, Netherlands

† Electronic Supplementary Information (ESI) available: See DOI: 10.1039/x0xx00000x

#Equally contributed authors

Corresponding Author Email: [venky@nus.edu.sg](mailto:venky@nus.edu.sg); [shaohorn@mit.edu](mailto:shaohorn@mit.edu)

## DESCRIPTION OF OWRK METHOD

In our work, wide range of samples ranging from hydrophilic to hydrophobic have been presented and therefore the OWRK method has been adopted which is suitable for universal systems.

The combining rule proposed by OWRK model is indicated below.

$$\gamma_{sl} = \gamma_{sv} + \gamma_{lv} - 2\left(\sqrt{\gamma_{sv}^D \gamma_{lv}^D} + \sqrt{\gamma_{sv}^P \gamma_{lv}^P}\right) \quad (1)$$

Where  $\gamma_{sv}^D$  and  $\gamma_{lv}^D$  are dispersive components and  $\gamma_{sv}^P$  and  $\gamma_{lv}^P$  are polar components of solid and liquid surface energies respectively.

Substituting for  $\gamma_{sl}$  from equation (1),

$$\sqrt{\gamma_{sv}^D \gamma_{lv}^D} + \sqrt{\gamma_{sv}^P \gamma_{lv}^P} = \frac{1}{2}[\gamma_{sv} + \gamma_{lv} - (\gamma_{sv} - \gamma_{lv} \cos\theta)] \quad (2)$$

$$\sqrt{\gamma_{sv}^D \gamma_{lv}^D} + \sqrt{\gamma_{sv}^P \gamma_{lv}^P} = \frac{1}{2}[\gamma_{lv}(1 + \cos\theta)] \quad (3)$$

By dividing  $\sqrt{\gamma_{lv}^D}$  in equation (4), we get,

$$\sqrt{\gamma_{sv}^D} + \sqrt{\gamma_{sv}^P} \frac{\gamma_{lv}^P}{\sqrt{\gamma_{lv}^D}} = \frac{1[\gamma_{lv}(1 + \cos\theta)]}{2\sqrt{\gamma_{lv}^D}} \quad (4)$$

The above equation can be represented in the linear form,

$$c + mx = y \quad (5)$$

where in,  $c = \sqrt{\gamma_{sv}^D}$      $m = \sqrt{\gamma_{sv}^P}$      $x = \frac{\gamma_{lv}^P}{\sqrt{\gamma_{lv}^D}}$

A graphical representation of the OWRK method is shown in Fig. S1 for sample 8 (lubricated hard disk media). The polar [SFTP(l)] and dispersive components [SFTD(l)] of total surface tension [SFT(l)] of the liquids used in this study are known (Table S1) and are substituted to compute the polar and dispersive components of the surface free energy of the solid. The slope of the graph gives the polar component and the vertical intercept gives the dispersive component of the solid surface free energy.

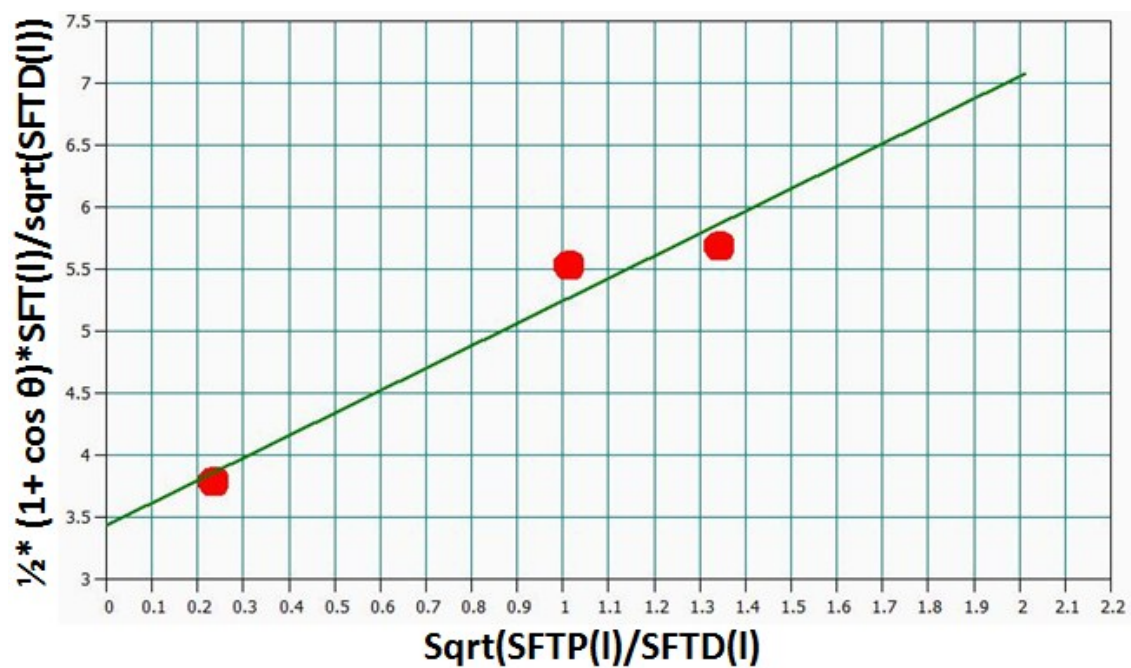


**Figure S1:** Surface energy (polar and dispersive) calculation graph based on OWRK model for sample 7 (lubricated hard disk media).

**Table S1:** Surface tensions of the test liquids

Label	SFT (Total) mN/m	SFT (Dispersive) mN/m	SFT (Polar) mN/m	Values Adapted From
Water	72.80	26	46.80	Gebhardt et al.
Ethylene Glycol	47.70	26.40	21.30	Gebhardt et al.
Diiodomethane	50.00	47.40	2.60	Busscher et al.

### DENSITY FUNCTIONAL THEORY CALCULATIONS

The adsorption energy of molecular and dissociated water, \*OH and \*H on the SrTiO<sub>3</sub>, VO<sub>2</sub> and Lu<sub>2</sub>O<sub>3</sub> has been computed by means of density functional theory (DFT) as implemented in the VASP code.<sup>[1]</sup> A Hubbard U term has been included on V *d* states and Lu *f* states ( $U_{\text{eff}}(\text{V}) = 3.25 \text{ eV}$  <sup>[2]</sup> and  $U_{\text{eff}}(\text{Lu}) = 5.4 \text{ eV}$ ,<sup>[3]</sup> respectively). We considered the (001) orientation of SrTiO<sub>3</sub>, both SrO and TiO<sub>2</sub>-terminated, and (022) of VO<sub>2</sub>(M) as they are expected to be the exposed film surfaces following the experimental indications. Note that SrTiO<sub>3</sub> sample preparation should result in a TiO<sub>2</sub>-terminated surface. The cubic bixbyite phase of Lu<sub>2</sub>O<sub>3</sub> expose preferentially the (111) surface, which has a large surface unit cell (16 Lu atoms per layer) and contains Lu ions with different local environment. We have then also considered the (0001) surface of hexagonal Lu<sub>2</sub>O<sub>3</sub> as a simplified model. This surface contains only fully coordinated Lu ions and has a lower surface energy compared to the cubic bixbyite (111) surface (by 0.26 J/m<sup>2</sup>), suggesting that the latter could reconstruct in order to minimize the number of under-coordinated cations. We can then infer that the two models represent the two extreme limits of surface reactivity, exposing reactive low-coordinated sites (cubic (111) surface) and less reactive fully coordinated cations (hexagonal (0001) surface). The adsorbate's binding energies have been computed in the low coverage regime (1/4 ML, where 1 ML would correspond to one adsorbate for surface metal atom) to assess relative stability of \*OH vs. H<sub>2</sub>O (both dissociated and molecular) on the oxide surfaces. In the case of cubic Lu<sub>2</sub>O<sub>3</sub>, this coverage has been obtained by placing four evenly distributed adsorbates per unit cell. The water binding energy is computed with respect to the gas phase H<sub>2</sub>O at 0.035 bar, while the \*OH and \*H binding energies are computed at 1.23 V with respect to the standard hydrogen electrode,<sup>[4]</sup> which corresponds to the H<sub>2</sub>O/O<sub>2</sub> equilibrium approximated to the ambient condition. The Gibbs free energies of the clean and adsorbate-covered surface have been computed by adding the zero point energy as estimated by vibrational analysis. The adsorption free energy has been defined as:  $G_{\text{ad}} = G(*X) - G(*) - \mu(X)$ , where  $G(*X)$  and  $G(*)$  represent the Gibbs free energy for the species X adsorbed on the surface and the clean surface respectively and  $\mu(X)$  is the chemical potential of X, defined as follow:

$$\mu_{\text{H}_2\text{O}(\text{g})} (= \mu_{\text{H}_2\text{O}(\text{l})}) = \mu_{\text{H}_2\text{O}(\text{g})}^0 + k_b \cdot \ln \left( \frac{p(\text{H}_2\text{O})}{p^0(\text{H}_2\text{O})} \right)$$

$$\mu_{\text{H}_2(\text{g})} = \mu_{\text{H}_2(\text{g})}^0 - 2e\phi + 2k_b T \cdot \ln(a_{\text{H}^+})$$

where  $\phi$  is the effective applied potential and the terms  $\mu_{\text{H}_2\text{O}(\text{g})}^0 = E_{\text{H}_2\text{O}(\text{g})}^{\text{DFT}} + \text{ZPE}_{\text{H}_2\text{O}(\text{g})} - TS_{\text{H}_2\text{O}(\text{g})}^0(0.035\text{bar})$  and  $\mu_{\text{H}_2(\text{g})}^0 = E_{\text{H}_2(\text{g})}^{\text{DFT}} + \text{ZPE}_{\text{H}_2(\text{g})} - TS_{\text{H}_2(\text{g})}^0$  have been determined from the computed DFT total energy (E), the zero point energy (ZPE) and the entropic translational, rotational and vibrational energy contributions at room

temperature. The chemical potential of H and OH are then defined as:  $\mu(\text{H}) = \frac{1}{2}\mu_{\text{H}_2(g)}$  and  $\mu(\text{OH}) = \mu_{\text{H}_2\text{O}(g)} - \frac{1}{2}\mu_{\text{H}_2(g)}$ .

The computed  $G_{\text{ad}}$  is reported in Fig. S2 for the modeled surfaces of (022) termination of  $\text{VO}_2(\text{M})$ , (001) SrO and  $\text{TiO}_2$  terminations of  $\text{SrTiO}_3$  (both), and hexagonal (0001) and cubic bixbyite (111) terminations of  $\text{Lu}_2\text{O}_3$ . For water both molecular and dissociative adsorption are reported, when stable. Spontaneous water dissociation was found on SrO-terminated  $\text{SrTiO}_3$  (001) surface, indicating that molecular water is not stable. Conversely, only molecular water is found on hexagonal  $\text{Lu}_2\text{O}_3$  (0001) surface, as the dissociated molecule readily recombines. In the case of cubic  $\text{Lu}_2\text{O}_3$  (111) surface the dissociated state corresponds to a mixed adsorption, with one molecular and three dissociated water molecules in the unit cell. Indeed on this surface the adsorption characteristics strongly depend on the specific adsorption sites and range from preferentially molecular at the fully coordinated Lu sites ( $G_{\text{ad}} = 0.33$  eV at 1/16 ML coverage) to dissociative at more exposed (low coordinated) Lu sites ( $G_{\text{ad}} = -0.27$  eV on the most stable adsorption site at 1/16 ML coverage).

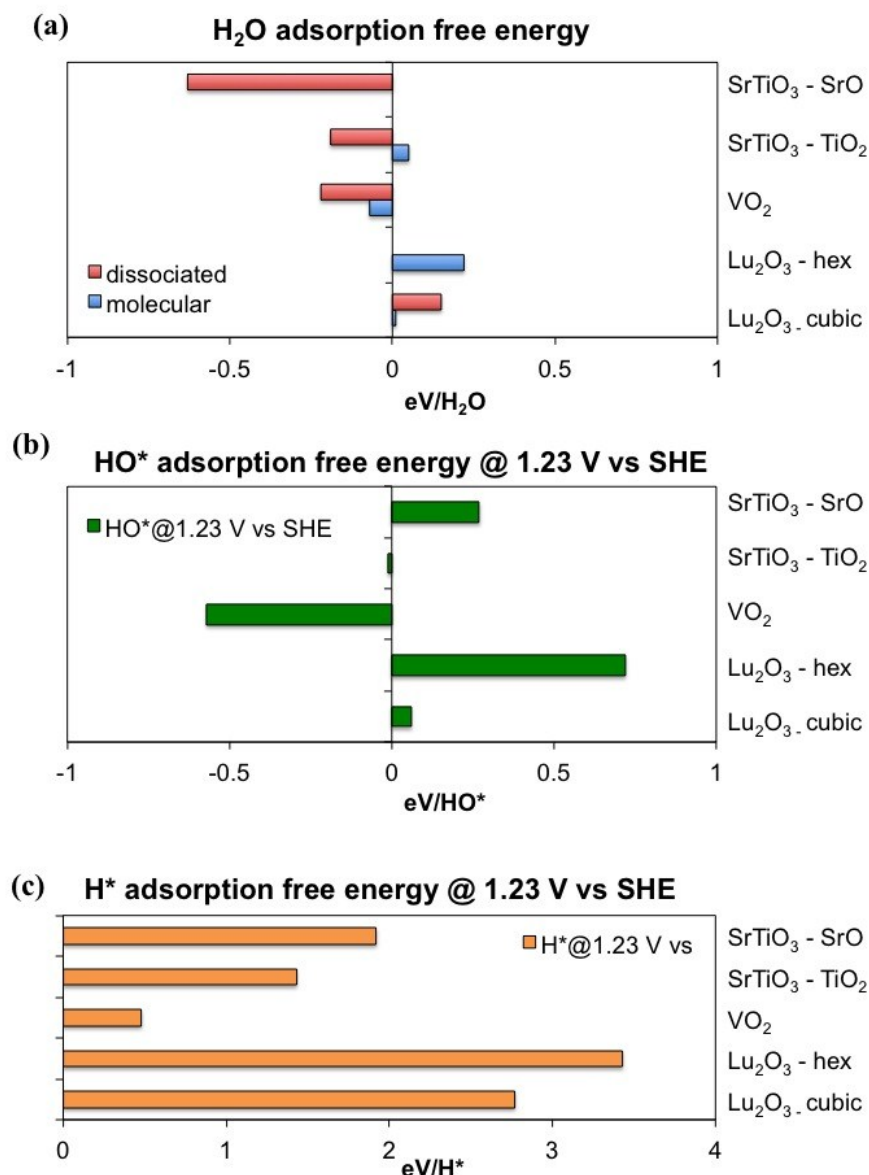


**Figure S2:** Computed adsorption free energies at 1.23 V with respect to the standard hydrogen electrode <sup>[4]</sup> for (a) H<sub>2</sub>O (molecular and dissociated), (b) \*OH and (c) \*H adsorbed on SrTiO<sub>3</sub> (001), VO<sub>2</sub>(M) (022), hexagonal Lu<sub>2</sub>O<sub>3</sub> (0001) and cubic bixbyite Lu<sub>2</sub>O<sub>3</sub>(111) surfaces computed at 1/4 ML coverage.

### Sample Preparation

Sample 1 (mica) was commercially procured.

Sample 2 & 3: Monoclinic VO<sub>2</sub>(B) and VO<sub>2</sub>(M) thin films on (100)SrTiO<sub>3</sub>(STO) substrates were grown using PLD respectively. The target was laser ablated using a pulsed KrF Excimer laser having a wavelength of  $\lambda = 248$  nm and pulse width of approximately 12 ns. The laser energy density was fixed at  $\sim 2$  J/cm<sup>2</sup> during the optimization of film growth parameters. The substrate temperature was kept 500° C throughout the deposition. At low pressure ( $1 \times 10^{-4}$  Torr) and 5 Hz laser rep rate, M phase is stabilized. At and above a pressure of  $5 \times 10^{-3}$  Torr and the laser rep rate to 2 Hz gave rise to a single phase VO<sub>2</sub>(B) film. The STO substrates were

cleaned by successively sonicating in acetone-deionized water-isopropyl alcohol-deionized water for 10 mins each.

Sample 4: Commercial hard disk media is Ar<sup>+</sup> ion etched to remove the conventional carbon overcoat. Hence the top surface is the CoCrPt based magnetic layer. (Though the top carbon layer is removed, it may contain traces of carbon.)

Sample 5: STO substrate was procured commercially from Crystec GMBH. The substrates were sonicated in DI water for 15 mins. After that the substrates were kept in buffered HF solution for 30 secs. They were subsequently washed with DI water and blow dried. The treated substrates were then annealed in the furnace at 950 °C for 2 hours. The ramp up rate was 5°/min and the ramp down rate was 3°/min.

Sample 6: Lu<sub>2</sub>O<sub>3</sub> film was grown using PLD technique. The target was laser ablated using a pulsed KrF excimer laser having a wavelength of  $\lambda = 248$  nm and pulse width of approximately 12 ns. The laser energy density was fixed  $\sim 2$  J/cm<sup>2</sup> during the optimization of film growth parameters. The substrate temperature was kept 750° C throughout the deposition. The pressure was 10<sup>-6</sup> Torr throughout the deposition.

Sample 7: Commercial hard disk media is Ar<sup>+</sup> ion etched to remove the conventional carbon overcoat and treated with high energy carbon using FCVA (Filtered Cathodic Vacuum Arc). Then the surface was treated with PFPE (Per fluoro polyether) based lubricant (Zdol 4000).

After fabrication, the samples were stored in a dry cabinet for a day. The samples were not subjected to any other handling, processing or measurement apart from the F-D measurement.

#### **Note on hydrocarbon contamination**

Hydrocarbon contamination is endemic to all surfaces exposed to ambient atmosphere. However, this does not matter as long as we have a homogeneous surface with well-defined wetting angle. The fact that our AFM measurements (done on different locations on the surface) correlate so well with the wetting angle measurement is an indirect proof of the homogeneity of the surfaces. We performed XPS on the Lu<sub>2</sub>O<sub>3</sub> sample. The data is shown below (Fig. S3). We have found that rare earth oxide surfaces pick up hydrocarbons far more than most other oxide surfaces and hence this data represents an upper limit to the carbon contamination in our oxide samples.

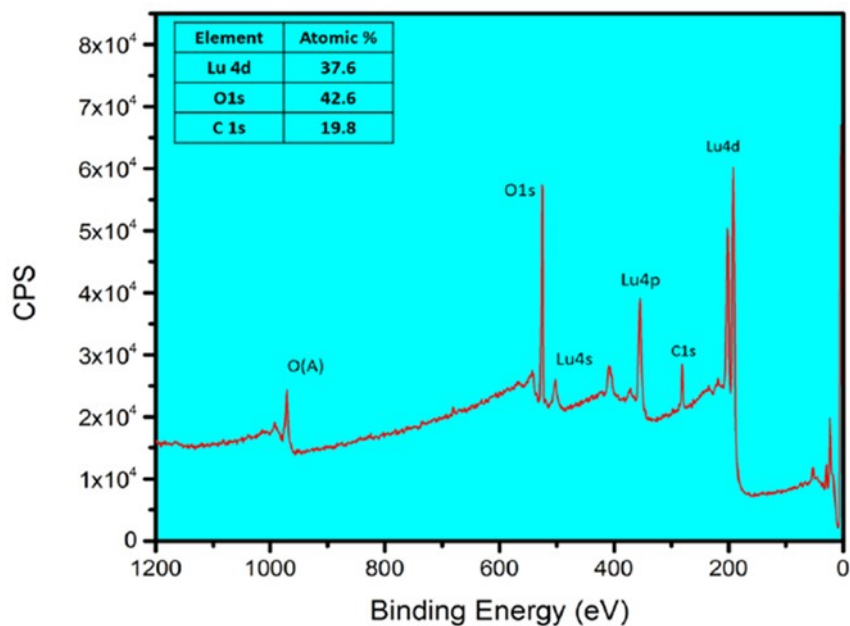


**Figure S3:** XPS spectra obtained from Lu<sub>2</sub>O<sub>3</sub> film.

#### Reproducibility of measurements made on the internal standard sample (lubricated hard disk media)

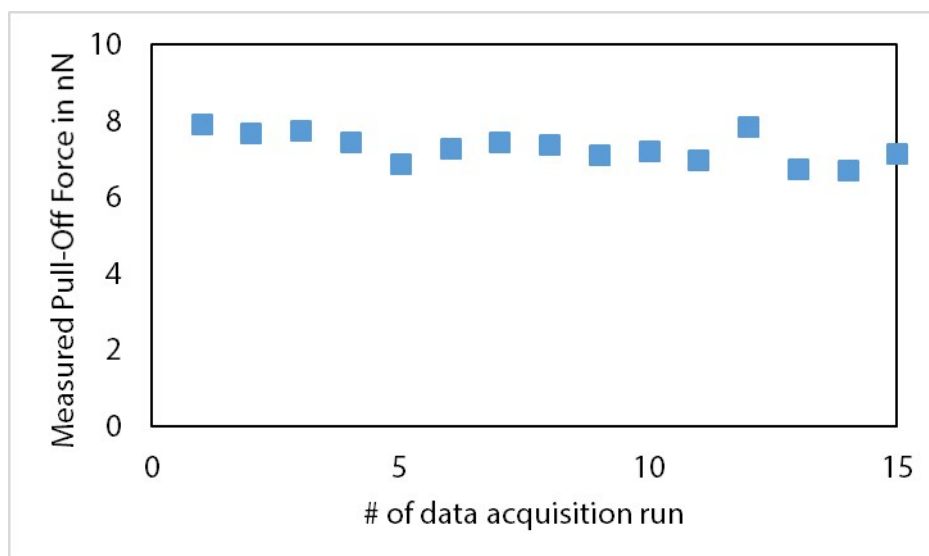


**Figure S4:** Pull-off forces obtained from LHM sample in between measurements of other samples.

We have repeated the study using another probe tip (a probe tip of <10 nm tip radius and 0.18 N/m spring constant). The data obtained from the new tip on three new samples [representatives for high (mica), low (lubricated hard disk media) and medium pull-off-force (hard disk media without lubricant)] are shown below (Fig. S5). The data shows the same trend as the original results in the manuscript and the force values are comparable as fortunately the RH values were similar (50-60%).

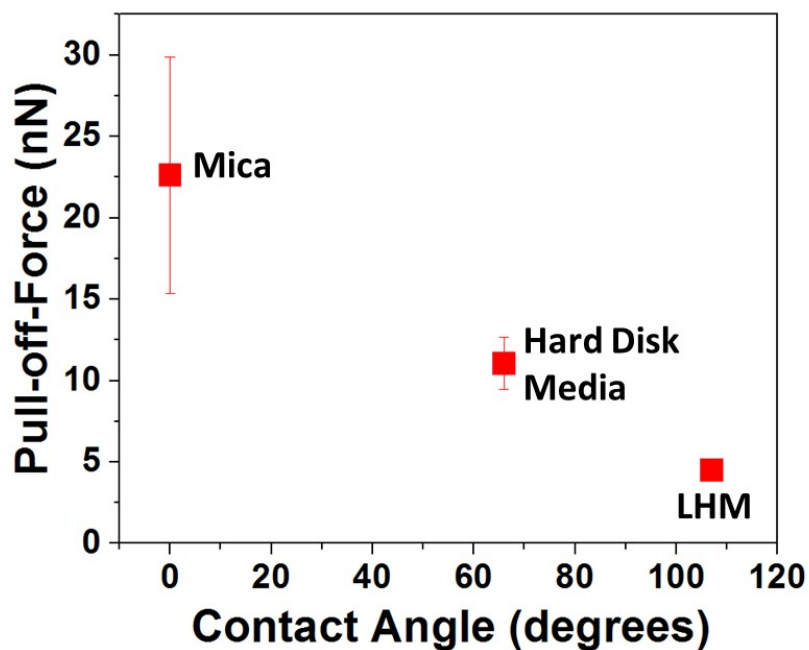


**Figure S5:** Water contact angle versus pull-of-force obtained on mica (0°), hard disk media (66°), lubricated hard disk media (107°) with another probe tip NANOSENSORS (Type PPP-CONT-20)

## References

- [1] G. Kresse, J. Furthmüller, *Phys Rev. B* **1996**, *54*, 11169.
- [2] L. Wang, T. Maxisch, G. Ceder, *Phys Rev. B* **2006**, *73*, 195107.
- [3] H. Jiang, R. I. Gomez-Abal, P. Rinke, M. Scheffler, *Phys Rev. Lett* **2009**, *102*, 126403.
- [4] J. K. Nørskov, J. Rossmeisl, A. Logadottir, L. Lindqvist, J. R. Kitchin, T. Bligaard, H. Jonsson, *J. Phys. Chem. B* **2004**, *108*, 17886-17892; bJ. Rossmeisl, Z. W. Qu, H. Zhu, G. J. Kroes, J. K. Nørskov, *J. Electroanal. Chem* **2007**, *607*, 83-89.